

Vortex Wall Dynamics and Pinning in Helical Magnets

Bahman Roostaei^{1,2}

¹ *Institut für Theoretische Physik, Universität zu Köln,
Zùlpicher Str. 77, D-50937 Köln, Germany and*

² *Department of Physics, Indiana University-Purdue University Indianapolis, Indiana 46202, USA*
(Dated: March 27, 2013)

Domain walls formed by one dimensional array of vortex lines have been recently predicted to exist in disordered helical magnets and multiferroics. Using a long wavelength approach supported by numerical optimization we lay out detailed theory for dynamics and structure of such topological fluctuations at zero temperature in presence of weak disorder. We show the interaction between vortex lines is weak. Also we show the internal degree of freedom of this array leads to the enhancement of its mobility. We present estimates for the interaction and mobility enhancements using the microscopic parameters of the system.

PACS numbers: 75.10.-b, 75.60, 75.70, 75.85

I. INTRODUCTION

Domain walls and domain patterns in magnetic materials to a large extent determine the controllability of the magnetic behavior of devices, a crucial factor in technology of today's spintronics and magnetic storage systems. Amongst various types of magnetic structures, helical magnets are in current interest demanding detailed studies of their properties under various circumstances. With the discovery of multiferroics¹, materials such as RMnO_3 in which $\text{R} \in \{\text{Y}, \text{Tb}, \text{Dy}, \text{Ho}\}$ ²⁻⁶ with coupled magnetic and electric properties and their intrinsic spiral magnetic order the necessity of such studies is understandable more than ever. A new class of topological domain walls has been predicted to exist in Helical magnets in recent studies⁷. These domain walls separate two anti-chiral domains and posses vorticity. These domains are indeed observed in circularly polarized X-ray scattering experiments¹⁰. Static domain patterns in these observations suggest strong pinning of the walls. In another recent study¹¹ the pinning mechanism of domain walls in these systems (Hubert walls) has been presented. Following this study, with an emphasis on pure vortex walls we present a detailed theory for structure and dynamics of these walls. We show that inside the topologically protected vortex walls⁷ the interaction between vortices is weak. We explain the effect of disorder on their structure and dynamics. We also explain how the internal dynamics of such walls can affect their mobility in presence of weak disorder. This is indeed a new realization of previously considered systems^{8,9} where internal degree of freedom enhances the mobility of the magnetic structure and therefore reduces the threshold force density.

We consider a major class of helical magnets, the centrosymmetric (CS) systems in which the magnetic moment distribution is invariant under space inversion. The helical axis in CS ground state is fixed. The Ginzburg-Landau hamiltonian density for helical CS magnets frequently used in literature can be written in the following

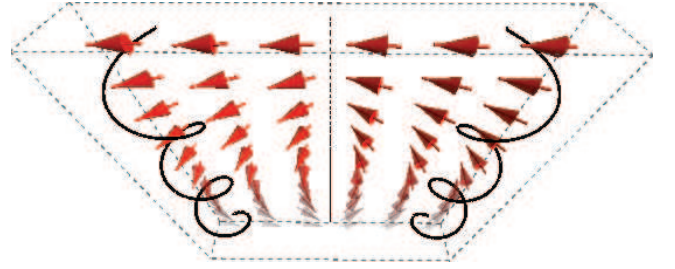


FIG. 1: Schematic illustration of the cross section of a vortex line (oval region) formed between two anti-chiral domains.

form:

$$h[\mathbf{m}] = \frac{J}{a} \left[(\partial_x^2 \mathbf{m} + q^2 \mathbf{m})^2 + (\nabla_\perp \mathbf{m})^2 \right] \quad (1)$$

in which the helical axis is dictated by the RKKY exchange anisotropy to be the \mathbf{x} axis.

II. VORTICES IN HELICAL MAGNETS

The existence of vortex domain walls in Helical magnets and multiferroics indicates the importance of a detailed analysis of vortex fluctuations in such systems. These systems are highly anisotropic as the system develops a ferromagnetic order in each easy plane and a helical order in the perpendicular direction. It is still possible to have vortex line excitations with the vorticity inside the easy planes. These vortex lines would consist of conventional vortices in each plane and their energy per unit length would be $\epsilon_\perp = J/a \log L/a$ in which L is the size of the ferromagnetic planes. On the other

hand there are vortex line excitations in which the direction of the vortex line is parallel to the easy planes and the structure of these vortices is not as simple as the former ones. In this case one needs to solve the non-linear saddle point differential equation associated with the hamiltonian (1) along with the boundary condition $\nabla \times \nabla \varphi = 2\pi\delta^2(\mathbf{r})\hat{\mathbf{z}}$. This has been performed before⁷ using an ansatz and separation of scales. In the next section we show that their result is also confirmed with numerical minimization. The variational approximation is used for different scales using a function of the form $\varphi = \tan^{-1}(\lambda y/x)$ which minimizes the energy by varying λ however we do this only for a certain distance r defined as: $r^2 = x^2 + \lambda(r)^2 y^2$. The result is⁷:

$$\varepsilon_v(r) = \frac{\pi J}{a^3} \log^{1/2}(r/a) \left[\frac{5}{64} + \theta^2 \log(r/a) \right]^{1/2} \quad (2)$$

and:

$$\lambda^2(r) = \theta^2 + \frac{5/64}{\log(r/a)} \quad (3)$$

For large enough $r \gg ae^{0.08/\theta^2}$ (the constant is not important since it comes from a variational calculation) the logarithmic term in the bracket dominates and the energy behaves logarithmic similar to conventional vortices in two dimensional XY models. For scales much less than this, close to the core of the vortex the value of the energy behaves as square root of logarithm. As the result this type of vortices in helical systems posses a layered structure.

III. VORTEX WALL

Another topological excitation possible in helical systems is vortex domain wall which is a one dimensional lattice of vortex lines parallel to the easy plane axes⁷. These walls separate antichiral domains from each other (see figure 1 for better imagination) . Using the same ansatz before one can introduce the following ansatz for the vortex wall:

$$\varphi(x, y) = \sum_{n=-N_v}^{N_v} \tan^{-1} \frac{\lambda y}{x - x_n} \quad (4)$$

in which $x_n = n\pi/q$ and $2N_v + 1 \gg 1$ is the number of vortex lines. This solution indeed satisfies the boundary conditions $\varphi(x, y) = \pm qx$ and $\partial_y \varphi = 0$ as $y \rightarrow \pm\infty$. This

can be seen by noting that for $N_v \gg 1$:

$$\begin{aligned} \partial_x \varphi &= \sum_{n=-N_v}^{N_v} \frac{-\lambda y}{(x - x_n)^2 + \lambda^2 y^2} \\ &= \frac{iq}{2} (\cot \bar{z} - \cot z) \end{aligned} \quad (5)$$

$$\begin{aligned} \partial_y \varphi &= \sum_{n=-N_v}^{N_v} \frac{\lambda(x - x_n)}{(x - x_n)^2 + \lambda^2 y^2} \\ &= \frac{q\lambda}{2} (\cot \bar{z} + \cot z) \end{aligned} \quad (6)$$

in which $z = q(x + i\lambda y)$. Clearly the above two expressions satisfy the boundary conditions.

From the above calculation it is interesting to observe that the field distribution close to the vortex wall is identical to the field of a single vortex:

$$\begin{aligned} \partial_x \varphi(z \rightarrow 0) &= \frac{iq}{2} \left(\frac{1}{\bar{z}} - \frac{1}{z} \right) = \frac{-\lambda y}{x^2 + \lambda^2 y^2} \\ \partial_y \varphi(z \rightarrow 0) &= \frac{\lambda q}{2} \left(\frac{1}{\bar{z}} + \frac{1}{z} \right) = \frac{\lambda x}{x^2 + \lambda^2 y^2} \end{aligned} \quad (8)$$

indicating that the value of the variational parameter in smaller scales will be identical to the value obtained for a single vortex but this would not be the case for larger length scales (see below). Moreover this is indicating the fact that the individual vortices in a vortex wall almost do not disturb each other in this variational solution, hence their interaction must be weak. This will be confirmed also numerically in the next section. It is very instructive to derive an analytic expression for the deformation energy of such vortex lattice as we proceed. The GL Hamiltonian for the low energy fluctuations of the vortex wall will be explained by $\mathbf{m}(\mathbf{r}) = \mathbf{e}_1 \cos \varphi(\mathbf{r}) + \mathbf{e}_2 \sin \varphi(\mathbf{r})$ and their energy density, using (1) is:

$$h = \frac{J}{a} \left\{ (\partial_\perp \varphi)^2 + \frac{a^2}{4} [(\partial_x \varphi)^2 - q^2]^2 + \frac{a^2}{4} (\partial_x^2 \varphi)^2 \right\} \quad (9)$$

In presence of the vortex wall at larger length scales we can write the effect of the wall deformations in the field as:

$$\partial_x \varphi = A_x(\mathbf{r}) + \psi \quad (10)$$

in which $A_x(\mathbf{r}) = q \text{sgn}_q[y - u_y(\mathbf{x}_\parallel)]$ is a smooth sign function which varies on the scales of q^{-1} and $u_y(\mathbf{x}_\parallel)$ is the position of the wall at each point of its plane and ψ is the remaining of the effects which is supposedly small. As the result up to second order in ψ we can write $[(\partial_x \varphi)^2 - q^2]^2 \approx 4q^2 \psi^2$. However we re-insert the full φ field into the Hamiltonian in order to preserve the non-perturbative effect of the vortices in the field:

$$h \approx \frac{J}{a} \left\{ (\partial_\perp \varphi)^2 + \theta^2 [\partial_x \varphi - A_x(\mathbf{r})]^2 \right\}. \quad (11)$$

Here we have ignored the highest derivative of φ assuming $\partial_x \psi \ll q\psi$. Introducing the rescaled coordinates $\tilde{\mathbf{r}} = \{x/\theta, y, z\}$ and fields $\tilde{\mathbf{A}} = \theta\{A_x, 0, 0\}$ we can write the above energy in the form of the vortex line lattice energy in a superconductor:

$$h \approx \frac{J}{a} \left[\tilde{\nabla} \tilde{\varphi} - \tilde{\mathbf{A}}(\tilde{\mathbf{r}}) \right]^2. \quad (12)$$

The saddle point equation from the above energy:

$$\tilde{\nabla} \cdot [\tilde{\nabla} \tilde{\varphi} - \tilde{\mathbf{A}}] = 0 \quad (13)$$

must be solved in presence of the vortices:

$$\tilde{\nabla} \times \tilde{\nabla} \tilde{\varphi} = \tilde{\mathbf{J}}(\tilde{\mathbf{r}}) \quad (14)$$

in which:

$$\mathbf{J}(\mathbf{r}) = 2\pi \sum_{n=-N_v}^{N_v} \int d\mathbf{r}_n \delta^3(\mathbf{r} - \mathbf{r}_n) \quad (15)$$

The solution to the above system can be obtained by introducing a vector potential:

$$\tilde{\nabla} \tilde{\varphi} = \tilde{\mathbf{A}} + \tilde{\nabla} \times \tilde{\mathbf{a}} \quad (16)$$

with a gauge freedom which we use by choosing $\tilde{\nabla} \cdot \tilde{\mathbf{a}} = 0$. Inserting this solution into (14) we obtain the equation:

$$\tilde{\nabla}^2 \tilde{\mathbf{a}} = \tilde{\nabla} \times \tilde{\mathbf{A}} - \tilde{\mathbf{J}} \quad (17)$$

which has the solution:

$$\tilde{\mathbf{a}}(\tilde{\mathbf{r}}) = \int_{\tilde{\mathbf{r}}'} G(\tilde{\mathbf{r}} - \tilde{\mathbf{r}}') [\tilde{\nabla}' \times \tilde{\mathbf{A}} - \tilde{\mathbf{J}}(\tilde{\mathbf{r}}')] \quad (18)$$

Inserting this solution into the energy we obtain:

$$\mathcal{H} = \theta \int_{\tilde{\mathbf{r}}, \tilde{\mathbf{r}}'} G_{\tilde{\mathbf{r}}\tilde{\mathbf{r}}'} [\tilde{\nabla} \times \tilde{\mathbf{A}} - \tilde{\mathbf{J}}(\tilde{\mathbf{r}})] \cdot [\tilde{\nabla}' \times \tilde{\mathbf{A}} - \tilde{\mathbf{J}}(\tilde{\mathbf{r}}')] \quad (19)$$

Let's calculate the vector $\Delta = \nabla \times \mathbf{A} - \mathbf{J}$ more explicitly. In order to do that we use the large scale approximation in which the density of the vortex lines is uniform :

$$\Delta(\tilde{\mathbf{r}}) = \frac{2\theta^3}{a^2} (\partial_z \tilde{u}_y \hat{\mathbf{y}} + \hat{\mathbf{z}}) [\delta_q(y - \tilde{u}_y) - \delta(y - \tilde{u}_y)] \quad (20)$$

this function is obviously non-zero only at a narrow region with the thickness q^{-1} of the order of the core of the vortices where our continuum approximation fails. The equation (19) clearly shows that the helical background represented by the vector potential screens the vorticity fields in large scales consistent with our choice of the ansatz (8).

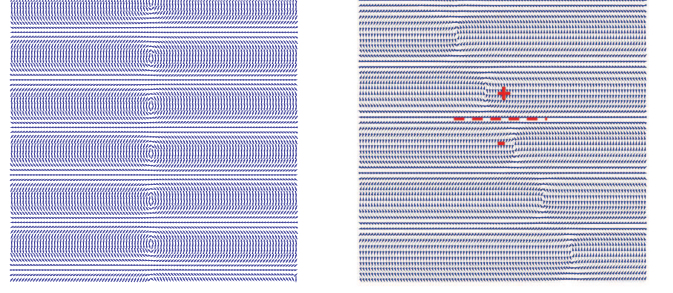


FIG. 2: Left: Vector field illustration of numerically optimized interface between two ani-chiral phases. Here $\theta = 0.32$. Right: Same as left but tilted. The plus/minus sign indicates the change in chirality hence existence of Hubert wall.

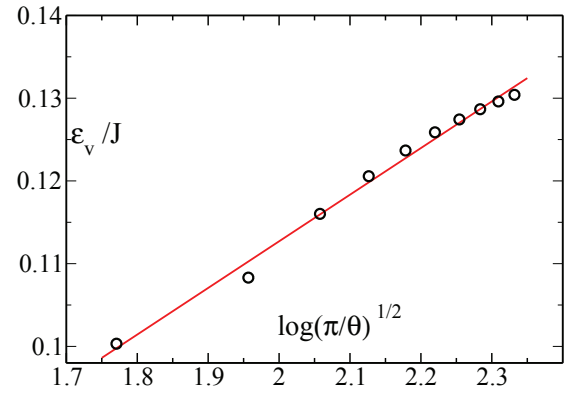


FIG. 3: Numerical comparison of the energy of the vortex domain wall per vortex(circles) with the results of the ansatz(solid line). The numerical result is obtained by optimization of the discrete model.

IV. NUMERICAL INVESTIGATION

For a more realistic investigation of the properties of vortex domain walls in helical magnets it is possible to use optimization techniques to find the lowest energy possible configurations of the discrete model at zero temperature. It is also possible to investigate the interaction between vortices in such configurations. In this section we show that the ansatz solution for the vortices obtained previously are in good agreement with optimized results in this section. Also we show that the interaction between vortices in a pure vortex wall are comparatively weak in agreement with our previous analytical speculations. We also justify the theory¹¹ for the tilt of vortex domain walls via generation of staircases of Hubert walls and vortex lines.

We use a two dimensional system with the assumption that the system is symmetric in the third direction i.e. the direction of vortex lines. We start with a configura-

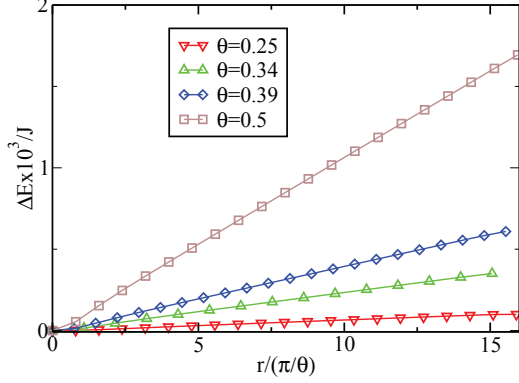


FIG. 4: Vortex interaction energy as a function of distance from the wall.

tion consisting of two helical domains with opposite chirality with a sharp interface between them and find the lowest energy possible using local iterative optimization methods. We use periodic boundary conditions in the direction of helical axis thus the number of the vortices in the wall is always even. For a wall with n vortices (see Fig.2) we find the total energy per unit of the length of the wall, $\ell_n = n\pi/\theta$ (in units of lattice constant and $J = 1$) obeys the following form:

$$\varepsilon_n = \alpha + \frac{\beta}{\ell_n} \sqrt{\log \ell_n} \quad (21)$$

fitting gives $\beta \approx 3.54$. This gives the energy of one vortex to be proportional to $(\log \pi/\theta)^{1/2}$ apart from an unimportant constant in agreement with the ansatz (Fig.3).

In order to make an estimate of the order of the interaction between these vortices in the wall we take the numerically obtained solution and displace one vortex out of the wall and obtain the minimum solution again by the same optimization technique (Fig.4). It is interesting to see that the energy difference between the two configurations is almost vanishing. This is a strong evidence that the vortices in the vortex wall almost do not interact and without pinning centers to hold the walls the domains may not exist.

The most elementary excitation of such wall based on the above results then are the formation of staircases¹¹. These staircases are consisting of vortices with a Hubert wall in between. It is easy to see this structure formation by considering a tilted array (see figure 2 right).

V. TILTED DOMAIN WALLS: STAIRCASE FORMATION

We showed in sections IV and III that the vortex lines in a vortex wall interact very weakly. A tilt of the vortex wall must then generate a staircase of vortex lines

of width π/q . Recently a theory for elasticity of vortex walls has been developed¹¹ based on *vicinal surface* approach. In this approach the elasticity of the vortex wall is found out to be local. Here for the sake of completeness we explain in more detail the derivation: Let's assume the tilt is around an axis parallel to ferromagnetic planes. This means the generated vortex lines are parallel to each other. The density of vortex lines for such a tilt with an angle α is $n(\alpha) = (q/\pi) \tan \alpha$. It is also important to remember that the energy of vortex lines in the system is distributed highly anisotropic (see sec.II, Eq. 2) so the energy of each vortex line would depend on α . As the result by adding the energies for the Hubert segments and the vortex lines (neglecting the vortex interactions) the energy density per unit of the area of the wall will be:

$$\sigma(\alpha) = \frac{\varepsilon_v(\alpha)n(\alpha) + \sigma_H}{\left(1 + \frac{n(\alpha)^2 \pi^2}{q^2}\right)^{1/2}} \quad (22)$$

$$= |\cos \alpha| \left(\frac{q}{\pi} \varepsilon_v(\alpha) \tan \alpha + \sigma_H \right) \quad (23)$$

In which σ_H is the elastic constant of the Hubert wall¹¹. Note that the energy density of a vortex line ε_v depends on α because of its anisotropic nature. A small tilt ϵ away from this configuration will cost an extra energy density to create vortex lines:

$$\begin{aligned} \Delta\sigma(\alpha, \epsilon) &= \frac{\sigma(\alpha + \epsilon)L(\alpha + \epsilon) - \sigma(\alpha)L(\alpha)}{L(\alpha)} \\ &= \sigma'(\alpha)|\epsilon| + \frac{1}{2}[\sigma(\alpha) + \sigma''(\alpha)]\epsilon^2 \end{aligned} \quad (24)$$

where $L(\alpha)$ is the linear size of the wall. The elastic energy of this wall then would be:

$$\mathcal{H}_e(\alpha) = \int d^2 \mathbf{r}_{\parallel} \Delta\sigma(\alpha, \epsilon(\mathbf{r}_{\parallel})) \quad (25)$$

Note that the linear term is zero at finite temperatures because the roughening transition temperature is almost vanishing¹¹. Above this temperature the vortices slide against each other almost freely so the average ϵ will be zero. With this fact we conclude that the total energy of the staircase is:

$$\mathcal{H}_e(\alpha) = \int d^2 \mathbf{r}_{\parallel} [c_1(\alpha)(\partial_x u)^2 + c_2(\alpha)(\partial_z u)^2] \quad (26)$$

which is local unlike Hubert walls¹¹. Note that the term $(\partial_z u)^2$ exist because of the area change of the wall upon tilting around x-axis. The elastic constants depend on the tilt of the domain wall and can be numerically calculated. The results are shown in figure 5.

VI. DISORDER

We consider a major type of disorder in this paper namely defects in crystals where magnetic atoms are

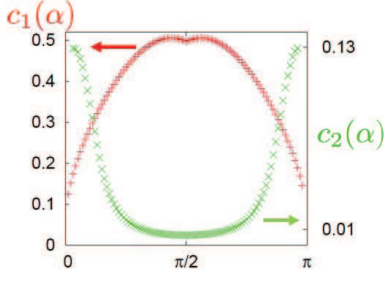


FIG. 5: Elastic constant of the vortex wall as the result of vicinal fluctuations as a function of orientation for $\theta = 0.5$.

missing on a particular site or a non-magnetic impurity is replaced by the magnetic atom. These defects are called vacancies. Usually domain walls gain exchange energy by adopting to these sites. In this case we attempt to derive a Hamiltonian for these types of disorder in continuum limit. Domain walls experience friction force due to these types of disorder. External driving forces can mobilize these walls provided they are stronger than a threshold value called depinning threshold. Periodic nature of the vortex walls however can have interesting behavior in presence of disorder and driving force. The internal lattice movement of the wall helps avoiding the pinning centers hence increasing the mobility of the walls above threshold value. Threshold values for both vortex wall and Hubert wall have been presented elsewhere¹¹. Here we explain the general theory in detail and show a new effect, *the enhancement of the mobility of the wall solely due to its internal degree of freedom*.

A. Dynamics of discrete domain walls

Here we discuss the dynamical aspects of such domain walls far from equilibrium in presence of external forces. We also show how it is possible to extract certain characteristics of domain walls such as Larkin length and depinning threshold. We show how a non-uniform density of a domain wall will result in the increase of effective mobility compared to generic values. Let's start with the overdamped equation of motion for each vortex line in the array:

$$\mu^{-1} \cdot \frac{\partial \mathbf{u}_n}{\partial t} = -\frac{\delta \mathcal{H}}{\delta \mathbf{u}_n} + \mathbf{f}(\mathbf{x}, \mathbf{u}_n) + \mathbf{h} \quad (27)$$

in which $\mathbf{u}_n = \{u_n(z), v_n(z)\}$ is the displacement vector of the vortex line number n with y and x components and:

$$\mathbf{f}(\mathbf{x}, \mathbf{u}_n) = -\frac{\delta \mathcal{H}_I}{\delta \mathbf{u}_n} \quad (28)$$

is the friction force density as the result of disorder. Here $\mathbf{x} = \{x, z\}$ representing a point on the wall. Also in the above \mathcal{H} is the elastic Hamiltonian of the wall determined

by equation (26) however throughout the rest of this calculation we assume the most general elastic Hamiltonian:

$$\mathcal{H} = \int_{\mathbf{k}} \hat{\mathcal{G}}_{\mathbf{k}} |\hat{\mathbf{u}}_{\mathbf{k}}|^2 \quad (29)$$

in which $\hat{\cdot}$ indicates the Fourier transformation. Finally \mathbf{h} is the deriving force density presumably applied uniformly across the wall. To determine \mathcal{H}_I , the disorder energy we use the fact that the wall consists of a one dimensional periodic array of vortex lines:

$$\mathcal{H}_I = \int_{\mathbf{r}} \mathcal{K}(\mathbf{r}) \mathcal{E}(\mathbf{r}) \quad (30)$$

in which:

$$\mathcal{E}(\mathbf{r}) = \sum_{n=-N_v}^{N_v} \epsilon_v[x - n\pi/q - v_n(z), y - u_n(z)] \quad (31)$$

and $\epsilon_v(x, y)$ is the energy density of a vortex line at point $\mathbf{r} = \{x, y, z\}$. The function $\mathcal{K}(\mathbf{r})$ determines the effect of disorder:

$$\mathcal{K}(\mathbf{r}) = \gamma \sum_{i=1}^{N_I} [f_I(\mathbf{r} - \mathbf{r}_i) - n_I] \quad (32)$$

with $f_I(\mathbf{r})$ being the vacancy/impurity form factor $\int_{\mathbf{r}} f_I(\mathbf{r}) = 1$ and n_I is their density. Throughout this article we assume the form factor vanishes in a range of the order of the crystal lattice constant. The sum in the above is over the position of impurities/vacancies \mathbf{r}_i which is random, γ is the effective volume occupied by impurity/vacancy, N_I is the number of impurity sites and $n_I = N_I/\Omega$ the impurity concentration. The above energy can be written as:

$$\begin{aligned} \mathcal{H}_I &= \int_{\mathbf{r}} \mathcal{K}(\mathbf{r}) \sum_n \epsilon_v[x - n\pi/q - v_n(z), y - u_n(z)] = \\ &= \int_{\mathbf{r}, \mathbf{r}'} \mathcal{K}(\mathbf{r}) \epsilon_v(x - x', y - y') \rho(\mathbf{r}') \\ &= \int_{\mathbf{r}} V(\mathbf{r}) \rho_v(\mathbf{r}). \end{aligned} \quad (33)$$

where we have defined:

$$V(\mathbf{r}) = \int_{\mathbf{r}'} \mathcal{K}(\mathbf{r}') \epsilon_v(x - x', y - y') \delta(z - z') \quad (34)$$

$$\rho_v(\mathbf{r}) = \sum_n \delta[y - u_n(z)] \delta[x - n\pi/q - v_n(z)] \quad (35)$$

as impurity potential and vortex line density. Here we approximate the vortex line density as if the displacement of vortex lines vary smoothly over the domain wall as the result we can treat the displacement vector as a smooth function of x : $\mathbf{u}_n(z) \approx \mathbf{u}(x, z)$. The impurity energy will be then of the following form:

$$\mathcal{H}_I = \int d^2\mathbf{x} V(\mathbf{x}, u_y) \rho(x - u_x) \quad (36)$$

where we have defined $\rho(x) = \sum_n \delta(x - n\pi/q)$. The force density vector has components perpendicular and parallel to the domain wall plane $\mathbf{f} = \{f_{\parallel}, f_{\perp}\}$:

$$f_{\perp}(\mathbf{x}, \mathbf{u}) = -\frac{\partial V}{\partial u_y} \rho(x - u_x) \quad (37)$$

$$f_{\parallel}(\mathbf{x}, \mathbf{u}) = V(\mathbf{x}, u_y) \rho'(x - u_x) \quad (38)$$

The goal is to find the force density \mathbf{h}_c at which the wall starts to move. However application of the most convenient tool namely perturbation in powers of disorder will only give us the force-velocity relation of the system at high velocities. While this approach will not ultimately lead to a relation in the full range of external force magnitudes it provides us with an estimate for the effective mobility of the system and also it will ultimately help us to estimate the threshold force density in large length scales in a renormalization group point of view¹². Let's now use the perturbation theory order by order to clarify the above argument: First we introduce the average drift velocity of the wall \mathbf{v} which in our case has only a non-zero component perpendicular to the domain wall plane $\mathbf{v} = v\hat{\mathbf{y}}$. The fluctuations out of the flat plane then can be separated:

$$\mathbf{u}(\mathbf{x}, t) = \mathbf{v}t + \boldsymbol{\xi}(\mathbf{x}, t) \quad (39)$$

On the other hand the disordered medium creates *static corrugations* with period q^{-1} in the wall:

$$\langle \boldsymbol{\xi}(\mathbf{x}, t) \rangle = \mathbf{g}(\mathbf{x}) \quad (40)$$

Here:

$$\langle A(\mathbf{r}) \rangle = \int \Pi_{i=1}^{N_I} \frac{d^3 r_i}{\Omega} A(\mathbf{r}, \mathbf{r}_i) \quad (41)$$

means averaging over disorder. This effect does not exist in more conventional Neel or Bloch type domain walls but here the periodic nature of the wall dictates such changes. This effect however is conventional in studies of pinned lattices¹³. We will present the resulting corrugation later in this section.

Now we expand the out of plane displacement in orders of disorder strength:

$$\boldsymbol{\xi} = \boldsymbol{\xi}^{(0)} + \boldsymbol{\xi}^{(1)} + \boldsymbol{\xi}^{(2)} + \dots \quad (42)$$

after averaging for the zeroth and first order we will have:

$$\boldsymbol{\mu}^{-1} \cdot \mathbf{v} = \mathbf{h} \quad (43)$$

$$\boldsymbol{\xi}^{(0)} = 0 \quad (44)$$

and:

$$\hat{\xi}^{(1)}(\mathbf{k}, \omega) = \int_Q \frac{\frac{-i\omega}{v^2} \hat{V}(k_x + Q, k_y, \frac{\omega}{v}) \hat{\rho}(-Q)}{i\mu_{\perp}^{-1}\omega + \hat{\mathcal{G}}_{\perp}^{-1}(\mathbf{k})} \quad (45)$$

$$\hat{u}_x^{(1)}(\mathbf{k}, \omega) = \int_Q \frac{\frac{-iQ}{v} \hat{V}(k_x + Q, k_y, \frac{\omega}{v}) \hat{\rho}(-Q)}{i\mu_{\parallel}^{-1}\omega + \hat{\mathcal{G}}_{\parallel}^{-1}(\mathbf{k})} \quad (46)$$

in which we have assumed the elastic energy for fluctuations parallel and transverse to the domain wall are governed by two distinct functions \mathcal{G}_{\parallel} and \mathcal{G}_{\perp} in the form of equation 29. For second order on the other hand:

$$\mathbf{f}(\mathbf{x}, \mathbf{u}) = \mathbf{f}(\mathbf{x}, \mathbf{v}t) + \boldsymbol{\xi} \cdot \nabla_{\mathbf{u}} \mathbf{f}(\mathbf{x}, \mathbf{v}t) \quad (47)$$

and after averaging:

$$\mu_{\perp}^{-1}v - h = - \int_{\mathbf{x}'} \mathcal{G}_{\perp}^{-1}(\mathbf{x} - \mathbf{x}') g_{\perp}^{(2)}(\mathbf{x}') + \langle \boldsymbol{\xi}^{(1)} \cdot \nabla_{\mathbf{u}} f_{\perp}(\mathbf{x}, \mathbf{v}t) \rangle \quad (48)$$

the second term on the right hand side depends only on x and is periodic consequently $g_{\perp}^{(2)}$ depends only on x and is periodic as well. Taking Fourier transform and

integrating over one period using the fact that $\hat{g}_{\perp}^{(2)}(0) = 0$:

$$\frac{\pi}{q} (\mu_{\perp}^{-1}v - h) = \int_{\mathbf{k}, \mathbf{Q}} \left[\frac{iQ_y^3}{\hat{\mathcal{G}}_{\perp}^{-1}(\mathbf{k}) - i\mu_{\perp}^{-1}Q_y v} + \frac{-iQ_y Q_x^2}{\hat{\mathcal{G}}_{\parallel}^{-1}(\mathbf{k}) - i\mu_{\parallel}^{-1}Q_y v} \right] |\hat{\rho}(Q_x)|^2 \hat{\Delta}(\mathbf{k}, Q_y) \quad (49)$$

in the above we have used the correlator function:

$$\Delta(\mathbf{r}) = \langle V(\mathbf{r})V(\mathbf{0}) \rangle = \gamma^2 n_I f_v(\mathbf{r}) \quad (50)$$

where:

$$f_v(\mathbf{r}) = \delta(z) \int dx' dy' \epsilon_v(x - x', y - y') \epsilon_v(x', y') \quad (51)$$

The depinning threshold naturally follows from setting $v \rightarrow 0$:

$$\frac{\pi}{q} h_c = \int_{\mathbf{k}, \mathbf{Q}} \left[-iQ_y^3 \hat{\mathcal{G}}_{\perp}(\mathbf{k}) + iQ_y Q_x^2 \hat{\mathcal{G}}_{\parallel}(\mathbf{k}) \right] |\hat{\rho}(Q_x)|^2 \hat{\Delta}(k_x - Q_x, k_z, Q_y) \quad (52)$$

$$= \int_{\mathbf{x}} \left[\mathcal{G}_{\perp}(\mathbf{x}) \Delta^{(3)}(\mathbf{x}, 0) C(x) + \mathcal{G}_{\parallel}(\mathbf{x}) \Delta^{(1)}(\mathbf{x}, 0) D(x) \right] \quad (53)$$

in which:

$$C(x) = \int_{x'} \rho(x') \rho(x - x') \quad (54)$$

$$D(x) = \int_{x'} \rho'(x') \rho'(x' - x) \quad (55)$$

and the derivatives of the correlator are introduced as follows:

$$\Delta^{(1)}(\mathbf{r}) = \langle \partial_y V(\mathbf{r}) V(\mathbf{0}) \rangle \quad (56)$$

$$\Delta^{(3)}(\mathbf{r}) = \langle \partial_y^3 V(\mathbf{r}) \partial_y V(\mathbf{0}) \rangle \quad (57)$$

Here we try to explain in details an approximate method used before¹¹ to estimate the threshold force density. The first assumption is that the correlator of disorder potential $\Delta(\mathbf{r})$ and its spatial derivatives are of short range with an average value of $\Delta_L^{(n)}$ (for n th derivative) at a length scale L . The length scale dependence comes from a renormalization point of view where one systematically sums up the contributions from smaller scales into the correlator using methods such as perturbation etc.¹² With this assumption and taking into account the fact that $D(x), C(x) > 0$ we arrive at the estimate for the threshold of force density at the length scale L :

$$h_c \approx \left[\mathcal{G}_{\perp}(L) \Delta_L^{(3)} + \mathcal{G}_{\parallel}(L) \Delta_L^{(1)} \right] \quad (58)$$

On the other hand for an isotropically distributed set of pinning centers, $\Delta^{(n)}$ is generically zero for odd n resulting in the zero threshold force density however it is well known¹² that in a renormalization group flow $\Delta_L^{(4)}$ develops a pole at scales larger than Larkin length scale \mathcal{L} where the energy gain due to collective weak disorder fluctuations can overcome the elastic deformation energy cost. This means $\Delta_L^{(2)}(\mathbf{x}, u)$ at $L \approx \mathcal{L}$ has a cusp near $\{\mathbf{x}, u\} = 0$ resulting in $\Delta_L^{(3)}$ being nonzero. The second term from the parallel deformations however remains zero at all length scales. Using this relation then one can estimate the threshold force density without having to worry about the physical value of the mobility. This will give us the maximum value possible because for scales higher than the Larkin length the disorder energy gain tends to decrease although it stays higher than deformation energy cost.

The above argument also leads us to a way to determine the Larkin length scale of the problem. Here we ignore the in-plane fluctuations of the wall and treat the vortex wall as a wall with uniform density. This will still give us the upper bound for the threshold force density because the internal fluctuations of the wall tends to reduce the magnitude of the threshold force as we will see at the end of this section. We start with the one-loop renormalization group flow equation for the force correlator $R(\mathbf{x}, u) = \langle f_{\perp}(\mathbf{x}, u) f_{\perp}(\mathbf{0}, 0) \rangle = -\Delta^{(2)}(\mathbf{x}, u)$. Provided we are close to the upper critical dimension we can use the renormalization group equation for R_L^{12} :

$$\begin{aligned} \frac{dR_L(u)}{dL} &= \mathcal{A}(L) \frac{d^2}{du^2} [R_L(u)(2R_L(0) - R_L(u))] \\ \mathcal{A}(L) \delta L &= \int_{1/L}^{1/(L-\delta L)} \frac{d^2 k}{8\pi^2} \hat{\mathcal{G}}^2(\mathbf{k}) \end{aligned} \quad (59)$$

taking two times derivative of the first equation in (59) and setting $u = 0$ and assuming $R_L^{(3)}(0) = 0$ as an analytic even function, we find the following solution up to the zeroth order in ϵ :

$$[R_a^{(2)}(0)]^{-1} - [R_L^{(2)}(0)]^{-1} = -6 \int_{1/a}^{1/L} \frac{d^2 k}{8\pi^2} \hat{\mathcal{G}}^2(\mathbf{k}) \quad (60)$$

in which $R_a(u)$ is at $L = a$ the bare correlation function. As was mentioned earlier this solution is divergent at the Larkin length given by the following equation at zeroth order of ϵ :

$$R_a^{(2)}(0) = \left[6 \int_{1/a}^{1/\mathcal{L}} \frac{d^2 k}{8\pi^2} \hat{\mathcal{G}}^2(\mathbf{k}) \right]^{-1} \quad (61)$$

In order to find the renormalized non-zero value of $R'(0) = \Delta^{(3)}(0)$ at Larkin length scale we need to use the functional renormalization group equation again. Assuming $\mathcal{A}(L) = A_0 L^{\gamma-1}$ we use the following ansatz:

$$R_L(u) = \alpha L^{-a} R^*(\beta u L^{-\zeta}) \quad (62)$$

The parameter α is fixed by the condition that the fixed point function $R^*(0) = 1$. Inserting this into the RG equation results in $a = -2\zeta + \gamma$ and:

$$R'_L(0) = L^{-\gamma/2} [R_L(0)]^{1/2} \left(\frac{-2\zeta + \gamma}{2A_0} \right)^{1/2} \quad (63)$$

On the other hand using the fact that $\int_{-\infty}^{+\infty} R_L(x)dx$ is invariant under the flow we obtain the exponent ζ with the physical assumption that $R^*(x) \rightarrow 0$ as $x \rightarrow \pm\infty$ to be $\zeta = \gamma/3$.

B. New effects in mobility correction

For the mobility itself on the other hand an interesting effect reveals when one calculates the effect of fluctuations of the wall internal structure. Using the real part of the equation (49) one can find a correction to mobility at non-zero velocity:

$$v = \tilde{\mu}_\perp h \quad (64)$$

$$\tilde{\mu}_\perp = \frac{\mu_\perp}{1 - \frac{q}{\pi} \ell_D} \quad (65)$$

in which:

$$\ell_D = \ell_\perp + \ell_\parallel$$

$$\ell_\perp = - \int_{\mathbf{k}, \mathbf{Q}} \frac{Q_y^4 |\hat{\rho}(Q_x)|^2 \hat{\Delta}(k_x + Q_x, k_z, Q_y)}{\left[\hat{G}_\perp^{-1}(\mathbf{k}) \right]^2 + (\mu_\perp^{-1} v Q_y)^2} \quad (66)$$

$$\ell_\parallel = \frac{\mu_\perp}{\mu_\parallel} \int_{\mathbf{k}, \mathbf{Q}} \frac{Q_y^2 Q_x^2 |\hat{\rho}(Q_x)|^2 \hat{\Delta}(k_x + Q_x, k_z, Q_y)}{\left[\hat{G}_\parallel^{-1}(\mathbf{k}) \right]^2 + (\mu_\parallel^{-1} v Q_y)^2} \quad (67)$$

Using the fact that $\hat{\Delta}(\mathbf{k}, Q) = \gamma^2 n_I |\hat{\epsilon}_v(kx, Q)|^2$ ($\hat{\epsilon}_v$ does not depend on k_z) is always positive one can see that $\ell_\perp < 0$ corresponding to the out of plane fluctuations of the wall trying to reduce the effective mobility of the wall while $\ell_\parallel > 0$ tries to increase it, an effect which depends on the gradient of the density of the wall (note the term $|Q_x \hat{\rho}(Q_x)|^2$ in the second equation). Also $\ell_\parallel = 0$ for uniform density. This is physically plausible since the lattice structure of the wall while driven, helps the wall to avoid resisting centers during its motion. Note that when $\mu_\parallel \rightarrow 0$ we have $\ell_\parallel \rightarrow 0$.

We can estimate the value of the above corrections by using proper cutoffs for large distance approximations and at high enough velocities. Those considerations leads us to the following approximation in units of lattice constant ($a = 1$):

$$\ell_\perp \approx n_I \gamma^2 \left(\frac{J\mu}{v} \right)^2 q^3 \quad (68)$$

$$\ell_\parallel \approx -n_I \gamma^2 \left(\frac{J\mu}{v} \right)^2 q^2 \quad (69)$$

In the above we have used $Q_x = 0$ mode of density to estimate the correction to mobility coming from transverse fluctuations and $Q_x = q$ to obtain the effect of the internal degree of freedom. Also we have made simplification by assuming $\mu = \mu_\perp \approx \mu_\parallel$ and used the previous approximations⁷ $\sigma_\perp \approx \sigma_\parallel \approx Jq/a$ in a quadratic elastic form.

C. Corrugation of The Vortex Wall

In this section we briefly analyze the structural properties of the domain wall in presence of domain wall. Our starting point is the equation (48) from which we can deduce the average displacement of the vortex wall at higher velocities. Since the second term on the right hand side of this equation is periodic the function $g_\perp^{(2)}(x)$ will have to be periodic as well. For simplicity we assume $\hat{G}_\perp = \sigma_\perp k^2$ and $\hat{G}_\parallel = \sigma_\parallel k^2$. After this consideration and some algebra one obtains for $g_\perp^{(2)}(x) = \sum_m g_m e^{imqx}$ the following:

$$g_m = \frac{c_m}{m^2} (1 - \delta_{m,0}) + \sum_{n \neq 0} \left[\frac{c_{m+n}}{m^2} + q^2 \frac{n(n+m)}{m^2} d_m \right] \quad (70)$$

in which:

$$c_m = \frac{\mu_\perp}{\sigma_\perp \pi^2} \int_{\mathbf{k}} \frac{-ik_y^3 \hat{\Delta}(\mathbf{k})}{\sigma_\perp \mu_\perp [k_z^2 + (mq - k_x)^2] - ik_y v}$$

$$d_m = \frac{\mu_\parallel q^2}{\pi^2 \sigma_\perp} \int_{\mathbf{k}} \frac{-ik_y \hat{\Delta}(\mathbf{k})}{\sigma_\parallel \mu_\parallel [k_z^2 + (mq - k_x)^2] - ik_y v} \quad (71)$$

Interestingly we see that the above coefficients are all zero for $v = 0$ which means the corrugations appear or enhance when the wall starts to move. It is also possible to estimate the value of the above integrals at the moving phase of the wall. Using $\hat{\epsilon}_v(\mathbf{k}) = -Jq/ak^2$ we will have:

$$c_{\pm 1} \approx d_{\pm 1} \approx n_I \gamma^2 \left(\frac{J\mu}{a^5 v} \right)^{1/2} q \quad (72)$$

where we have the same simplifications as previous section for mobility and elastic constants. Also in the above we have used a cutoff for the integral over k_x to include only wavelength of the order of q^{-1} . Finally smaller wavelengths ($|m| > 1$) in the corrugation have been neglected for large scale approximations.

VII. DISCUSSION AND CONCLUSIONS

In this paper we have presented an analytic model as well as numerical verification of the predicted vortex walls in both clean and disordered helical magnets. From an analytic point of view we showed how the helical background screens the vorticity effect in long distances resulting in the weak interaction between vortex lines. We have also presented a detailed discussion of the dynamics of such wall in the presence of disorder. Using established renormalization group ideas we have explained in detail how it is possible to theoretically predict the threshold force density for domain walls in general. In this calculation we have also shown that a moving vortex wall

array will display on average *spatial corrugations*. In this discussion we have also revealed how the periodic nature of the wall will result in correction of the mobility toward higher values compared with other conventional magnetic domain boundaries. Here we can further discuss such effect by time scale considerations. The time scale during which a domain wall with a thickness of $\sim q^{-1}$ passes a pinning center during its motion is of the order of $\tau_{\perp} \sim q^{-1}/v$. On the other hand the effect of this impact throughout the wall propagates during a time scale $\tau_{\parallel} \sim \lambda^2/\sigma_{\parallel}\mu_{\parallel}$ in which λ is the length of propagation. The ratio of the two time scales then will be: $\tau_{\parallel}/\tau_{\perp} \sim \theta(\lambda/\xi_{\parallel})^2$ in which $\xi_{\parallel} = (\sigma_{\parallel}\mu_{\parallel}a/v)^{1/2}$ is the typical correlation length between fluctuations throughout the wall. In order for the periodic nature of the wall have any effect in the dynamics of the wall the propagation length must be at least of the order of the period of the vortex line array $\lambda \sim q^{-1}$. These considerations result in a range of velocities $v \leq v_p \sim \sigma_{\parallel}\mu_{\parallel}q$

at which the periodic effect show up. This will then directly determine the range of external force densities $h \leq h_p = v_p/\mu_{\perp} \sim \sigma_{\parallel}q\mu_{\parallel}/\mu_{\perp}$ at which the periodic structure affects the motion of the wall. This value of h_p can be used in experiments to study the nature of the boundaries between anti-chiral domains.

Acknowledgments

I would like to thank Prof. Thomas Nattermann for his critical supervision, Institute for Theoretical Physics at the University of Cologne in Germany for hosting most of this work and Sonderforschungsbereich 608 for financial support. Also I would like to thank Prof. Yogesh N. Joglekar and the Indiana University-Purdue University at Indianapolis for their support.

-
- ¹ S. Cheong and M. Mostovoy, Nature Mat. **6**, 13 (2007).
² M. Kenzelmann et. al, Phys. Rev. Lett. **95**, 087206 (2005).
³ S. Picozzi, et. al, J. Phys. Cond. Matt. **20**, 434208 (2008).
⁴ T. Kimura, et. al., Nature **426**, p. 55 (2003).
⁵ T. Arima, et. al., Phys. Rev. Lett. **96**, 097202 (2006).
⁶ D. Talbayev, et. al., Phys. Rev. Lett. **101**, 247601 (2008).
⁷ F. Li, T. Nattermann and V.L. Pokrovsky, Phys. Rev. Lett.**108**, 107203 (2012).
⁸ S. S. Parkin, M. Hayashi, and L. Thomas, Science **320**,

- 190 (2008).
⁹ V. Lecomte, S. E. Barnes, J.-P. Eckmann, and T. Giamarchi, Phys. Rev. B **80**, 054413 (2009).
¹⁰ J.C. Lang et al., J. Appl. Phys. **95**, 6537 (2004).
¹¹ T. Nattermann, arXiv:1210.1358
¹² T. Nattermann et al., J. de Physique (1992).
¹³ S. Brazovskii and T. Nattermann, Advances in Physics **53**, 177-253 (2004).